J Mater Sci (2007) 42:7787–7793
DOI 10.1007/s10853-007-1646-2

# Effect of liquid phase on densification in electric-discharge compaction

**Xiyong Wu · Jingdong Guo**

Received: 9 June 2006 / Accepted: 27 February 2007 / Published online: 3 June 2007


**Abstract** The effect of liquid phase on densification in electric-discharge compaction (EDC) was explored in the present work. The temperature at contact area of particles in EDC was estimated from random packing model incorporated with electric current distributions. Consolidation of cemented carbide and tungsten heavy alloys was conducted under varying current densities. WC-11Co/Fe/WC-11Co sandwich powder compacts were designed to investigate the effect of liquid phase flow. It is found that the densification occurred only when liquid phase formed, and relative density increased with the increasing of liquid phase volume. In the case of WC-11Co powders, the faceted grain evolution occurred but the significant grain growth was hardly observed, which meant the densification was mainly induced by particle rearrangement. The depth of liquid penetration of Fe in WC-11Co/Fe/WC-11Co sandwich compact also agreed with that caused by particle rearrangement processing. The possible effects of electric current on densification were also discussed.

## Introduction

In recent years, numerous processes have been developed that apply an external electrical current to assist materials processing, such as powder wire discharge [1], mechanical alloying [2], powder consolidation [3–8], chemical synthesis [9] and solidification [10]. The idea to use electrical current in sintering was proposed by Taylor early in 1933 [11], termed ''electrical resistance sintering under pressure''. In 1950s, metal powders and cemented carbide powders were consolidated by passing high amperage current through the material at synchronous pressure [12]. More recently, various consolidation techniques have been developed using the effect of electrical current to enhance driving force in sintering and shorten sintering time. The current assisted sintering techniques can be classified into two kinds: the electric-discharge compaction (EDC) [6] and numerous variants of the field-activated sintering technique (FAST) [7] including spark plasma sintering (SPS), plasma-activated sintering (PAS), and pulse electric current sintering (PECS). In the former case, the electrical energy is suddenly released by discharging a capacitor bank through a powder compact within about one millisecond. In the latter case, a typical pulse discharge is used by the application of a low voltage (~30 V) and high current (~1,000 A), the duration of each pulse varying from 1 to 300 ms and the holding time about several minutes.

Although FAST and EDC have been successfully applied to a variety of powder consolidation, including metals, ceramics and composites, only considerable numbers of studies were focused on the possible mechanism of FAST and EDC. Groza [7] considered that the physical activation of initial particle surface due to the spark in FAST eliminated the surface impurities and enabled the necessary cohesion of grain boundary. The sparks among the copper particles were also observed at contact areas during a single-pulse electric discharge [13]. Mamedov proposed that the main densification mechanisms in SPS were viscose flow and plastic yielding, as shown in hot isostatic press (HIP) or hot pressing (HP) [14].

X. Wu · J. Guo (✉)
Shenyang National Laboratory for Materials Science,
Institute of Metal Research, Chinese Academy of Sciences,
72 Wenhua Road, Shenyang 110016, China
e-mail: jdguo@imr.ac.cn

In EDC processing, the surface effects, such as breakdown of surface oxide film, were also observed, and the neck formation and growth in EDC processing was studied [6, 15, 16], but the effect of diffusion, viscose flow and creep should be little due to the short holing time. Therefore, there may be other factors contributed to densification.

In this work, the liquid phase effect on densification in EDC is explored, the typical liquid phase sintered materials such as cemented carbides and tungsten heavy alloys selected. Furthermore, the temperature in particle contact area is estimated by modeling and the liquid flow in EDC is investigated from WC-11Co/Fe/WC-11Co sandwich compacts, the effects of electric current on densification also discussed.

## Experimental procedure

The spherical iron powder, tungsten heavy alloys with nickel-to-iron ratios of 7:3 and coarse-grained WC-11 wt% Co powders were used in this study. The tungsten content in tungsten heavy alloys was varying as follows: 90 wt%W–Ni–Fe, 95wt%W–Ni–Fe and 98wt%W–Ni–Fe. The schematic illustration of EDC system was described previously [17]. One gram loose powders without additives were placed into the insulator die with diameter 5.5 mm under external pressure up to 300 MPa. The relative density of powders under pressure was about 60%. The powders under pressure were discharged from a 360 μF capacitor with different current densities. The waveform of EDC was detected in situ by a Rogowski coil and a digital storage oscilloscope (TDS3012, Tektronix Inc., Beaverton, OR), the typical waveform of EDC presented in Fig. 1. The density of sample was measured by the Archimedes' principle. The morphologies of compacts were observed under a scanning electron microscope (SEM). WC-11Co/Fe/WC-11Co sandwich powder compacts were designed to investigate the effect of liquid phase flow, the scheme of compacts shown in Fig. 2. The microstructure of WC-Co powders and iron powders was shown in Fig. 3. The WC grain size in WC-11Co powders and iron powders is about 3 and 2 μm, respectively. The depth of Fe penetration into WC-11Co compacts under EDC was measured from WC-11Co/Fe interface using electron probe microanalysis (EPMA).

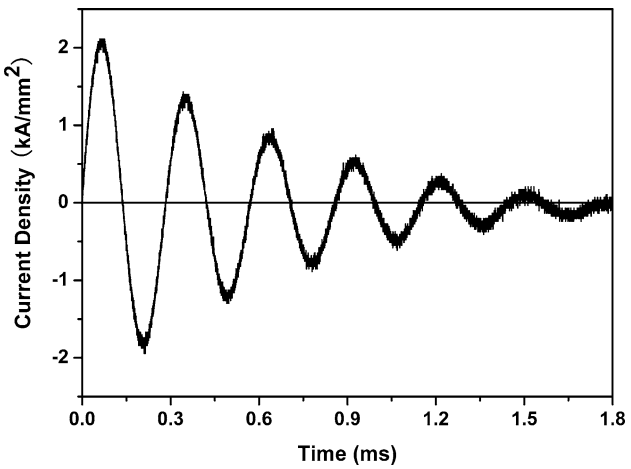


**Fig. 1** Typical waveform in EDC

## Results and discussion

### Temperature at contact area

Due to the short holding time and the necking formation [15], the temperature distribution at inter-particle contact area is essential in EDC. We incorporate electrical current

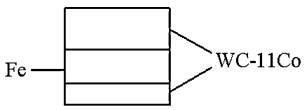


**Fig. 2** Scheme of sandwich powders WC-11Co/Fe/WC-11Co

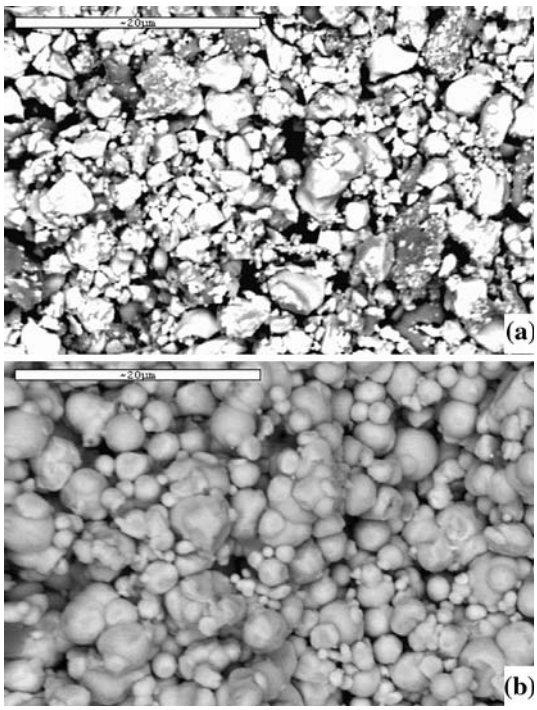


**Fig. 3** SEM of WC-11Co powders and Fe powders: (**a**) WC-11Co powders (**b**) Fe powders

distributions into the random packing model described in literature [18–20] to estimate the temperature at contact area. The assumptions are as follows:

(1) Under pressure, the incompressible particles are randomly packed spheres with initial radius $R_0$ in an aggregate and initial relative density $D_0$.
(2) At contact area, the Joule heat during discharge is not dissipated by heat radiation or conduction.
(3) Before the peak current ($I_p$) arrives, the particle surface is purified due to surface effect of electric field and the action time on surface clean is much shorter than discharge time. It was in conformity with the reports that a dramatic decreasing in resistance of compact was observed before $I_p$ arrived [21, 22].
(4) Electrical current with the same current density in the direction of $I$ only flows into one half of a particle and flows out from the other half of the particle through inter-particle contact area, as shown in Ref. [13].

According to Arzt's work, the average coordination number in the pressing limit is [18]

$$\begin{aligned} Z(D) &= Z_0 + 9.5(D - D_0) \quad \text{for } D < 0.85 \\ Z(D) &= Z_0 + 2 + 9.5(D - 0.85) + 881(D - 0.85)^3 \\ &\quad \text{for } D > 0.85 \end{aligned} \tag{1}$$

where $Z(D)$ is the average coordination number, $D$ the relative density, and $Z_0 = 7.3$ is the average initial coordination number of packing.

The average contact area in the pressing limit is as follows [18]:

$$a(D) = 3R_0^2(D - D_0) \text{for } 0.7 < D < 0.95 \tag{2}$$

The current flowing through one particle is [13]

$$\frac{\pi R^2 J}{D} = \sum_1^{Z/2} aj\cos\theta = aj\sum_1^{Z/2}\cos\theta = aj\frac{Z}{2}\overline{\cos(\theta)} \tag{3}$$

where $\theta$ is the spatial angle between the normal direction of the contact zone and the direction of $I$, $J$ the current density measured by oscilloscope in experiment, and $j$ the microscopic electrical current density at interparticle contact area, as shown in Ref. [13]. The current density at contact area is higher than that in the particle, and then the liquid phase forms at contacts preferentially.

The temperature of each contact area can be calculated [23]:

$$\Delta T_i = \int_0^{t_p} [j\cos(\theta_i)]^2 \rho/(\mathrm{d}c)\mathrm{d}t \tag{4}$$

where $\rho$ is the resistivity, $d$ the density of bulk materials, $t_p$ the pulse time and $c$ the specific heat.

From Eq. 4, the temperature at each contact area could be obtained. Due to the different angle between normal direction of contact area and electrical current, the temperatures are different at contact areas. At the contact area perpendicular to electric current, the temperature is the highest; while the temperature at the contact area parallel to current is nearly zero. This analysis of temperature distribution is confirmed by the observation of continuous fibrous structures aligned in the direction of current flow [21].

For simplicity, we propose the average contact temperature of a particle defined as follows:

$$\Delta T = \overline{\Delta T_i} = \sum_1^{Z/2} (\cos\theta_i)^2 \int_0^{t_p} j^2\rho/(\mathrm{d}c)\mathrm{d}t \tag{5}$$

For iron, taking $\rho$ = 50 nΩ m, $d$ = 7.87 g cm$^{-3}$, and $c$ = 486 J kg$^{-1}$ K$^{-1}$ [24], the Eq. 5 is presented in Fig. 4. It is shown that the temperature is sensitive to the relative density and increases with the increasing of current density dramatically at low density. For WC-Co cemented carbides, only Co melts and spreads along the surface of particle, therefore the average temperature of contact area can be estimated with the parameter of Co here. Taking $\rho$ = 62.4 nΩ m, $d$ = 8.8 g cm$^{-3}$, and c = 440 J kg$^{-1}$ K$^{-1}$ [24], the current density needed for formation of cobalt liquid is about 1.0 kA mm$^{-2}$ at relative density of 70%. For W–Ni–Fe alloys, taking $\rho$ = 64 nΩ m, $d$ = 8.88 g cm$^{-3}$, and c = 460 J kg$^{-1}$ K$^{-1}$ [24], the current density needed

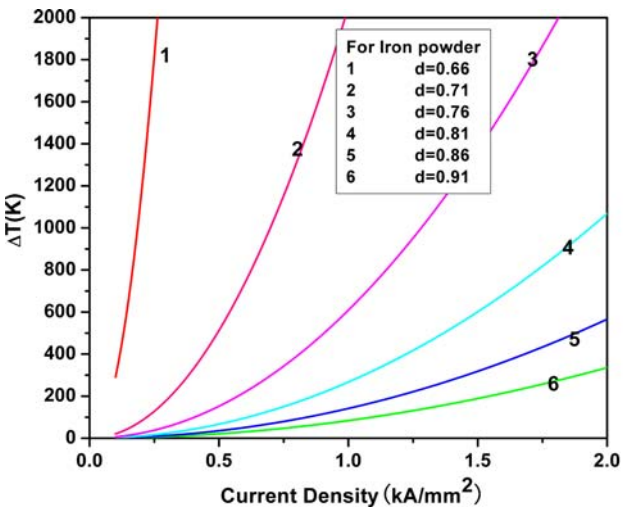


**Fig. 4** Temperature at contact area of Fe compacts at different relative density

for formation of Ni-Fe liquid is about 1.0kA $mm^{-2}$ at relative density of 70% estimated by the same method.

## Densification in EDC

From temperature estimation at contacts stated above, it is shown that the liquid phase of binder, such as Co and Ni–Fe, is formed first in EDC processing of WC-Co cemented carbides and W–Ni–Fe alloys, respectively. In liquid phase sintering (LPS) densification was primarily governed by processes like particle rearrangement and solution-reprecipitation [25]. The particle rearrangement occurs instantaneously after liquid formation, approximately 0.01 s [25, 26], and is localized to the particle contact regions when the capillary force is greater than the inherent solid-phase strength. Increasing the capillary force or reducing the inherent solid-phase strength between contacts will enhance densification by particle rearrangement [26, 27]. The high temperature at contact areas may reduce the inherent solid-phase strength; while a higher liquid phase fraction or external stress increase the driving force [27]. Solution-reprecipitation which includes solid dissolution into the liquid and solid leaving the liquid by precipitation on existing grains is dominant in LPS. Grain growth always occurs in parallel with densification during solution-reprecipitation controlled by diffusion or interface reaction. To explore the densification mechanism in EDC with formation of liquid phase, the effect of liquid phase volume on densification, microstructure evolution in WC-Co cemented carbides and depth of liquid flow are presented as follows.

W–Ni–Fe alloys with varying W contents, e.g., 98W–Ni–Fe, 95W–Ni–Fe and 90W–Ni–Fe, are consolidated to investigate the effect of liquid phase volume on densification. The current density in experiments is about 2.5 kA $mm^{-2}$. For 98W–Ni–Fe, nearly no effect of densification in EDC occurs and the compacts are even broken when taking out from the die. For 95W–Ni–Fe and 90W–Ni–Fe powders, densification is achieved obviously. The maximum density of 95W–Ni–Fe obtained is about 14 g $cm^{-3}$, while that of 90W–Ni–Fe is about 16 g $cm^{-3}$ in the experiments. The microstructure of 98W–Ni–Fe after EDC does not distinguish much from that of initial powders, as shown in Fig. 5a. The SEM of powders and compacts of 90W–Ni–Fe are shown in Fig. 5b and c, the effect of densification presented obviously. The Ni–Fe pockets are also identified in Fig. 5c, which indicates the formation of liquid phase. These results show that densification only occurs with enough liquid phases.

In the case of WC-11Co cemented carbide powders, Fig. 6 shows that the relative density of the compacts increases with the increment of current density before the critical value, and is retard beyond this value, similar

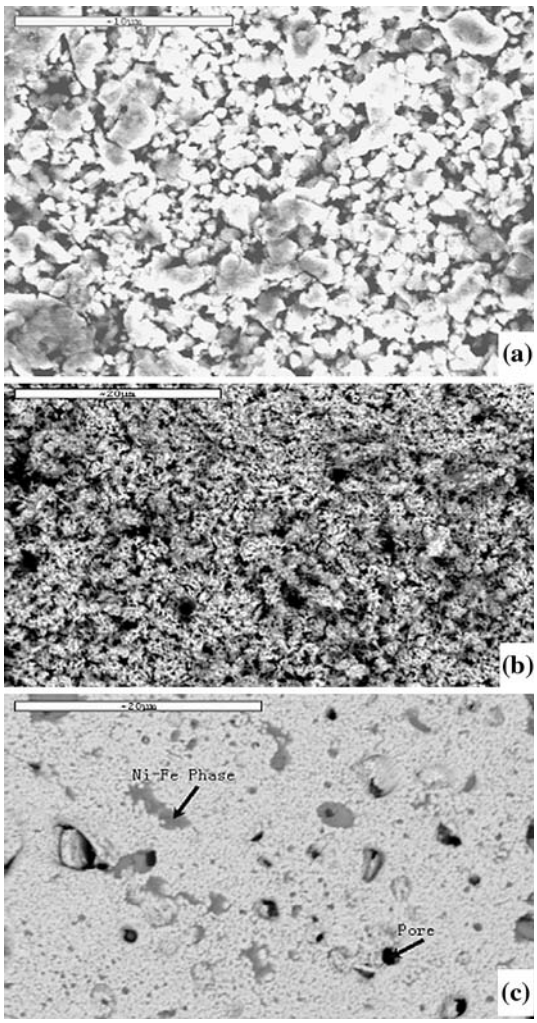


**Fig. 5** SEM investigations of W-Ni-Fe powders and compacts (**a**) 98W–Ni–Fe compacts after EDC (**b**) 90W–Ni–Fe powders (**c**) 90W–Ni–Fe compacts after EDC

results also reported in literature [21]. With the increment of current density in EDC processing of WC-11Co, the more paths of electrical current form at compacts and more Co liquid phase occur at particle contacts, which also indicate that densification increases with increasing of liquid phase volume.

The microstructure evolution of WC grains with different current densities is shown in Figs. 7–9. At current density of 1.8 kA $mm^{-2}$, the WC grains are round as the initial particles in compacts without EDC. With the increment of current density up to 2.1 kA $mm^{-2}$, the faceted WC grains occur and more faceted WC grains are shown when current density raised to 2.5 kA $mm^{-2}$. The average grain size of WC is about 3 ~ 3.5 μm in EDC compacts, as shown in Figs. 7b–9b. Comparing with that of WC powders shown in Fig. 3a, grain growth of WC in EDC processes is slight, and significant grain growth with the increment of current density also not observed.

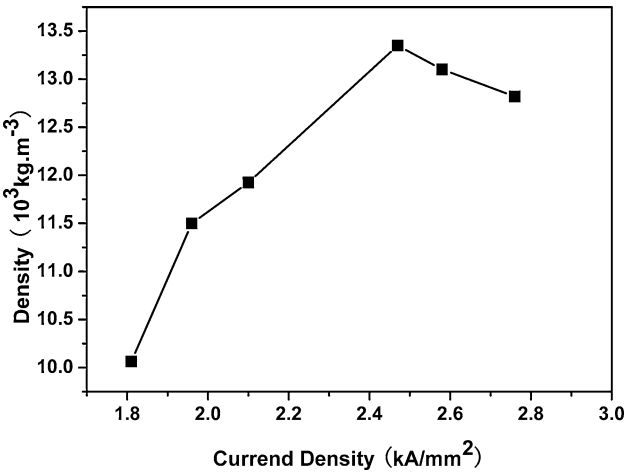


**Fig. 6** Densification of WC-11Co powders with different electric current density

WC has a highly anisotropic structure and therefore faceted grains are developed in dissolution of WC in Co during particle rearrangement and subsequent solution-reprecipitation processing, which does not occur in LPS of W–Ni–Fe alloys and only round grains are observed in W–Ni–Fe powders and sintered materials. When pulse electric current passes, Co liquid phase forms at contact

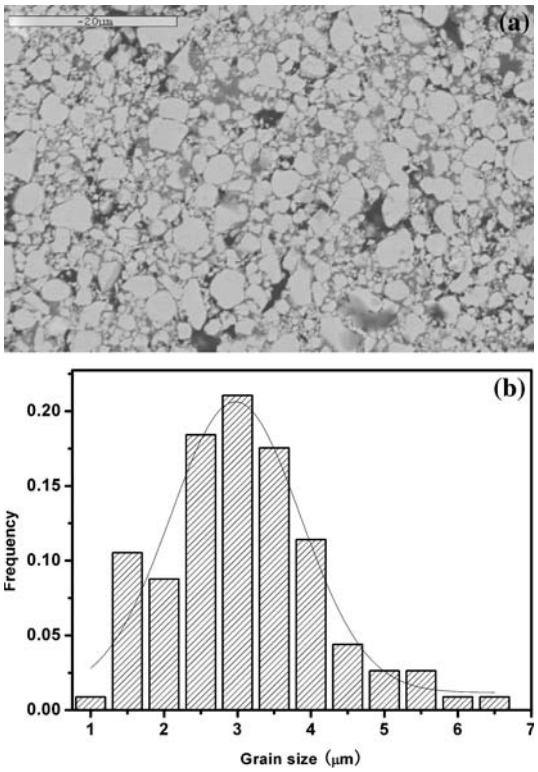


**Fig. 7** (**a**) Microstructure of WC-11Co powders after EDC at 1.8 kA mm$^{-2}$ and (**b**) the corresponding grain size distribution for WC phase

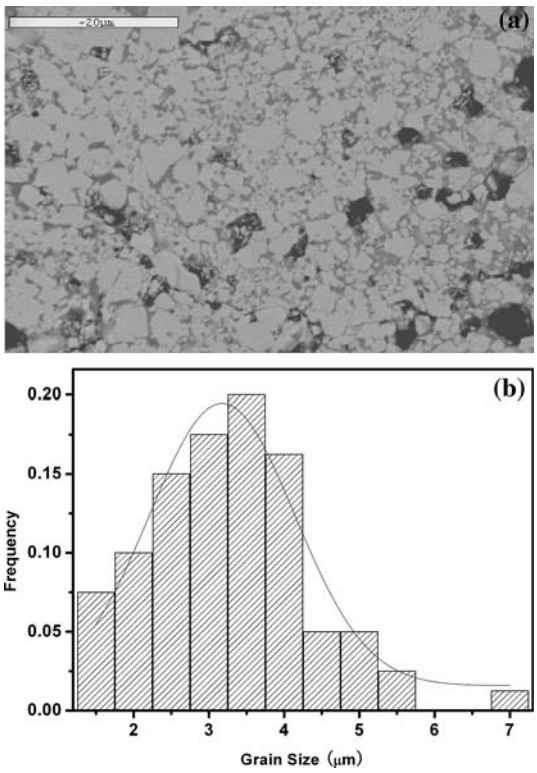


**Fig. 8** (**a**) Microstructure of WC-11Co powders after EDC at 2.1 kA mm$^{-2}$ and (**b**) the corresponding grain size distribution for WC phase

area in particle compacts and the dissolution of solid in liquid phase also increases with the increment of liquid phase volume. Therefore with the increasing of electrical current density in EDC, the fraction of Co liquid phase also increase and more WC are dissolved in binder phase, then more faceted grains are formed as revealed in Figs. 8 and 9. Since the solution-reprecipitation in WC-Co is controlled by interface reaction, dissolution of WC in binder phase is fast compared with precipitation of dissolved amount. From the dissolution rate constant of WC in Co phase reported by Lavergne [28], which is $1.6 \times 10^{-5}$ m s$^{-1}$, the thickness of WC dissolution in binder phase at one dimension is about 16 nm in this work, which is slight compared with the grain size mentioned above. It is apparent that the dissolution of WC is limited and solution-reprecipitation processing is constrained. The discharge time is also comparable with the time scale in particle rearrangement. So, the faceted grain shown in experiment may be formed only during particle rearrangement by dissolution of WC in binder phase.

Furthermore, the depth of liquid flow in EDC processing is investigated from WC-Co/Fe/WC-Co sandwich compacts shown in Fig. 2, the results given in Table 1 and Fig. 10. The depth of liquid penetration increases with the increasing of the current density or voltage, from 100 μm

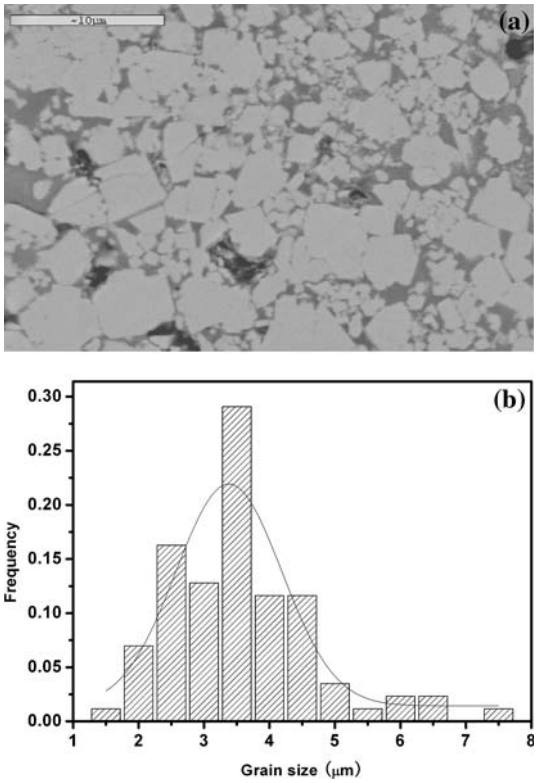


**Fig. 9** (**a**) Microstructure of WC-11Co powders after EDC at 2.5 kA mm$^{-2}$ and (**b**) the corresponding grain size distribution for WC phase

**Table 1** Distance of Fe penetration in WC-Co cemented carbide

| Voltage (kV) | Current density (kA/mm$^2$) | Distance (μm) |
|---|---|---|
| 4.8 | – | 100 |
| 5.4 | 1.96 | 250 |
| 6.0 | 2.20 | 400 |

at 4.8 kV to 400 μm at 6.0 kV. In particle rearrangement processing, the penetration depth is expressed as [25]:

$$x = \sqrt{\frac{d_p \gamma_{LV} t \cos(\theta)}{4\eta}} \tag{6}$$

where $x$ is the depth of liquid penetration, $d_p$ the pore size, $\gamma_{LV}$ the liquid–vapor surface energy, $\theta$ the contact angle, $t$ the time, and $\eta$ the liquid viscosity. For Fe in WC-Co compacts, taking $d_p$ = 3 μm as the pore size, $\gamma_{LV}$ = 1.9J m$^{-2}$, $\theta$ = 0, $\eta$ = 5.5 mPa s [29], and $t$ = 1 ms, the depth of liquid phase penetration obtained is about 400 μm, which is in agreement with the results in our experiment. From above analyses, it is proposed that solution-reprecipitation is

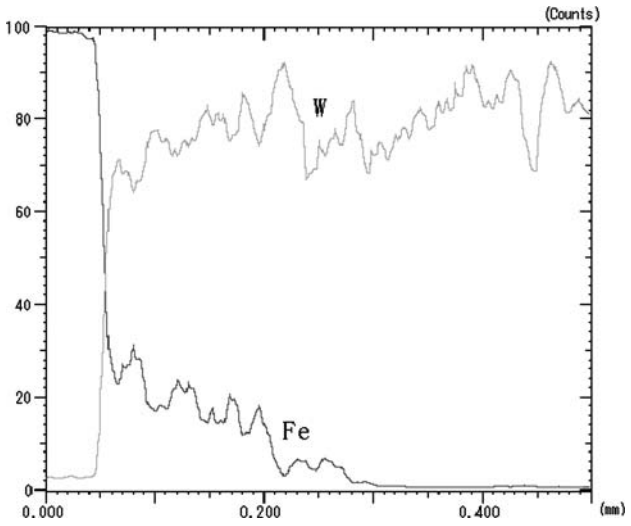


**Fig. 10** EPMA of WC-11Co/Fe interface

slight and particle rearrangement maybe the main densification mechanism in EDC.

In conventional liquid phase sintering, the inherent solid-phase strength in compact is formed at solid state sintering stage or heating period [24]. Due to the rapid heating in EDC processing, the solid state sintering is suppressed and the inherent solid-phase strength which retarded particle rearrangement is reduced. When pulse electrical current flow the compacts, electrical current paths and liquid phase are formed at particle contact area due to the least resistance, liquid phase flowing in porous compacts. Then densification by particle rearrangement occurs and grain growth by solution-reprecipitation is restricted. So it is possible to consolidate nanometer powders by EDC to achieve ultrafine grain size with high density [17].

## Effect of electrical current

In EDC processing, the compacts are heated internally by pulse electrical current, which is different from external heating in conventional furnace methods, such as HP, HIP, and LPS. Besides the heating effect, the electrical current may also affect densification. The possible effects are discussed as follows.

(1) *Pinch effect* The pinch effect in EDC was investigated by Okazaki et al. and Alp et al. [21, 22]. In cylindrical powder column, the pinch effect was given by: $F = \frac{\mu}{4} j^2 (a^2 - r^2)$, where $a$ is the radius of the cylindrical conductor, $\mu$ the permeability, and $r$ the distance from the center of the column. The pinch effect induces the powder compacts to be compressed radially with a porous layer [16].

(2) *Effect on vacancies diffusion* Vacancies diffusion induced by electric field was explored in Conrad's work [30], which showed that the density was higher near the surface from the cross section view of the compacts.

(3) *Effect on liquid flow* The effect of electrical current on liquid flow was investigated by Raichenko [31]. It was shown that the electrical current promoted motion of the liquid phase deeper into pores and other such defects, such as aluminum in graphite perform [31]. A clean understanding of the mechanism of this effect was not at hand. The electrical current may decrease the viscosity of liquid phase in sintering [32], or affect the flow of liquid metal in porous bodies due to their effect on the surface of liquid metal [33].

In SEM investigation of WC-Co compacts after EDC, the difference of porosity between the center of compact and near the surface is not observed (the pictures not shown here), which means that the effect of pinch effect and the vacancies diffusion on densification is not significant, or the pinch effect counteracts the effect on vacancies diffusion in this work. From the experiment of WC-Co/Fe/WC-Co EDC processing, it is shown that the electric current enhances the penetration of liquid phase of iron into WC-Co porous compacts. Besides the effect of high temperature in EDC which affects viscosity and volume of liquid phase, the effects of pulse electric current on liquid flow may also work. Due to the short holding time in EDC, the temperature of Fe is difficult to obtain directly. Further work is needed to reveal the effect of electric current on densification.

## Conclusion

The effect of single pulse electric discharge on powder compaction was investigated from EDC of W–Ni–Fe powders and WC-Co powders. The results were summarized as follows.

(1) The temperature at contacts was estimated from random packing model incorporated with electric current distributions, which was sensitive to the green density of compacts and increased rapidly with the increasing of electric current density at lower density.

(2) The densification in EDC only occurred with enough liquid phases. In this processing, solution-reprecipitation was slight and particle rearrangement may be the main densification mechanism.

(3) The effect of electrical current or electric field, such as pinch effect and the effect on vacancies diffusion, was not significant in our experimental observations.

**Acknowledgements** Financial supports by the National Natural Science Foundation of China (Nos. 50371091 and 90206044) and National Major Basic Research Development Program Item of China (2002CB613503) are acknowledged. Prof. G. H. He and Dr. X. L. Wang are greatly acknowledged for their valuable help.

## References

1. Jiang W, Yatsui K (1998) IEEE Plasma Sci 26:1498
2. Calka A, Wexler D (2002) Nature 419:147
3. Mishra RS, Mukherjee AK (2000) Mater Sci Eng 287A:178
4. Omori M (2000) Mater Sci Eng 287A:183
5. Newman DC (2000) Mater Sci Eng 287A:198
6. Okazaki K (2000) Mater Sci Eng 287A:189
7. Groza JR, Zavaliangos A (2003) Rev Adv Mater Sci 5:24
8. Rajagopalan PK, Desai SV, Kalghatgi RS, Krishan TS, Bose DK (2000) Mater Sci Eng 280A:289
9. Feng A, Munir ZA (1995) Metall Mater Trans 26B:587
10. Conrad H (2000) Mater Sci Eng 287A:205
11. Taylor GF (1933) U.S. Patent No. 1896854
12. Lenel FV (1955) J Metal 7:158
13. Yanagisawa O, Kuramoto H, Matsugi K, Komatsu M (2003) Mater Sci Eng 350A:184
14. Mamedov V (2002) Powder Metall 45:322
15. Yavuz N, Can M (1997) J Mater Proc Manu Sci 5:197
16. Ana YB, Oha NH, Chuna YW, Kima YH, Kima DK, Parkb JS, Kwonc J-J, Choid KO, Eomd TG, Byund TH, Kime JY, Reucroftf PJ, Kimg KJ, Lee WH (2005) Mater Lett 59:2178
17. Wu XY, Zhang W, Wang W, Yang F, Min JY, Wang BQ, Guo JD (2004) J Mater Res 19:2240
18. Arzt E (1982) Acta Metall 30:1883
19. Helle AS, Easterling KE, Ashby MF (1985) Acta Metall 33:2163
20. Swinkels FB, Wilknson DS, Arzt E, Ashby M (1983) Acta Metall 31:1829
21. Alp T, Al-Hassani STS, Johnson W (1985) J Eng Mater Tech 107:186
22. Kim DK, Pak H, Okazaki K (1988) Mater Sci Eng 104A:191
23. Sprecher AF, Mannan SL, Conrad H (1983) Scri Metall 17:769
24. Shackelford JF, Alexander W (2001) Materials science and engineering handbook. CRC Press LLC, p 597
25. German RM (1996) Sintering theory and practice. John Wiley & Sons Inc., p 270
26. Liu J, German RM (2001) Metall Mater Trans 32A:3125
27. Xu K, Mehrabadi MM (1997) Mech Mater 25:137
28. Lavergne O, Allibert CH (1999) High Temp High Press 31:347
29. Battezzati1 L, Greer AL (1989) Acta Metall 37:1791
30. Fahmy Y, Conrad H (2001) Metall Mater Trans 32A:811
31. Raichenko AI, Istomina TI, Popov VP, Derevyanko AV, Vishnyakov LR, Moroz VP (2003) Powder Metall Metal Ceram 42:213
32. Peng H (2004) Ph.D Thesis, Stockholm University
33. Zon BA (2001) Phys Lett 292 A:203